# BAW Phase Velocity Measurements by Conventional Pulse Echo Techniques with Correction for Couplant Effect

B.T. Sturtevant, M. Pereira da Cunha
Dept. of Physics and Dept. of Electrical Engineering
Laboratory for Surface Science and Technology
University of Maine, Orono, Maine USA
mdacunha@eece.maine.edu

*Abstract*— **This work reports on the importance of considering the couplant between a fused silica buffer rod and the piezoelectric sample in pulse echo overlap measurements. A transmission line model is used to account for the couplant effect in the measurement of bulk acoustic wave (BAW) phase velocities. The couplant correction theory and the experimental procedure and setup are detailed in this paper. Experiments have been performed with quartz and langatate (LGT). Quartz, due to its well-known material properties, has been used to validate the experimental procedure and confirm the necessity of considering the couplant effect. On LGT, BAW phase velocities have been measured along ±45° Y rotated cuts, and the X, Y, and Z crystalline axes for the extraction of the full set of elastic constants. The experiments revealed that the effect of the couplant accounts for a correction to the measured BAW phase velocities about one order of magnitude above other experimental uncertainties. Corrections for the phase velocity measurements on quartz and LGT of the order of $10^{-3}$ have been verified, which indicate the relevance of the couplant correction in pulse echo based parameter extraction.**

**Keywords-** *LGT; elastic constants; pulse echo measurements*

## I. INTRODUCTION

The accurate extraction of acoustic wave constants and their respective temperature coefficients is a critical step in the determination of crystal cuts for bulk and surface acoustic wave (BAW and SAW) device applications. The design and fabrication of bulk and surface acoustic wave (BAW and SAW) devices requires an accurate set of constants and their respective temperature coefficients.

The pulse echo overlap (PEO) technique has been used for almost six decades as a method of determining the bulk acoustic wave velocities for both isotropic and anisotropic solids [1, 2]. This work reports on the consideration of the couplant in the measurement of BAW phase velocities used for the extraction of the elastic constants of piezoelectric crystals. The technique is based on the analysis outlined in [3, 4] to correct the measured BAW phase velocities, $v_p$.

Two materials have been used in this work: quartz and $La_5Ga_{5.5}Ta_{0.5}O_{14}$ (langatate, LGT). Quartz was selected to validate the experimental technique, due to its well known acoustic properties. PEO measurements of BAW in quartz have been performed along the X, Y, Z crystalline axes. The second material used in this work, LGT, is a very attractive piezoelectric material, which exhibits temperature compensated orientations, piezoelectric coefficients between two to three times higher than quartz, and capability of operation at high temperatures, due to the inexistence of crystalline phase transitions up to its melting point [5-8]. With such favorable properties, a reliable set of acoustic constants and temperature coefficients for the prediction of application oriented LGT cuts is thus highly desirable. For LGT, PEO measurements of BAW were taken along five axes: X, Y, Z, Y±45°, Euler angles $[\Phi,\Theta,\Psi]$= [0°, ±45°, 90°]. The rotated Y cuts were chosen in order to extract the $C_{13}$ and $e_{14}$ constants. From the extracted BAW phase velocities, the material's elastic and piezoelectric constants were calculated by a method similar to that of [9]. The results obtained in this work confirm the relevance of considering the couplant in providing corrections around $10^{-3}$ in PEO measurements.

Section **II** reviews the PEO technique and discusses the motivation for the couplant correction technique employed. Section **III** describes the experimental procedure including equipment used in the collection and processing of data. Section **IV** presents the room temperature elastic constants determined in this work. Finally, Section **V** concludes the paper.

## II. REVIEW OF MEASUREMENT TECHNIQUE AND INTRODUCTION TO COUPLANT CORRECTION

In the PEO technique, an acoustic wave pulse is introduced to a sample by way of a piezoelectric transducer. Between the transducer and the sample, a fused silica buffer rod is commonly used to clearly identify the pulse reflection from the front face of the sample. At both the buffer rod/couplant/sample and sample/air interfaces, the pulse undergoes reflections (Fig 1a.). Figure 1b shows the experimental setup used in this work. The return times of the various reflections are recorded on an oscilloscope and compared to determine the time of flight of the pulse in the sample. The phase velocity of the AW is calculated by dividing the path length, 2L (Fig 1a), by the time of flight. In Fig. 1a, the arrows depict the path traveled by the pulse and the planes at which reflections occur. When possible, we compare the time of arrival of pulse B and B'. The difference in the time taken for these two signals to return, $\Delta t'$, is given by [4]:

Funding for this project was provided by the Army Research Office ARO Grant # DAAD19-03-1-0117, by the Petroleum Research Fund Grant ACS PRF# 42747-AC10, and by National Science Foundation NSF Grant # DGE-0504494.

$$\Delta t' = \Delta t + \frac{\Phi_{R31}}{2\pi f} \quad (1)$$

where Δt is the transit time in the sample, $f$ is the carrier frequency of the pulse, and $\Phi_{R31}$ is the phase delay introduced when B reflects off the sample/couplant/buffer rod interface (the reflected portion of B is then called B') as in Fig 1a. In some cases, it is impossible to compare pulses B and B' because the geometry of the sample and the phase velocity are such that B' interferes with a second reflection at the buffer rod/couplant/sample interface (not shown in diagram). In this event, it is necessary to compare pulses A' and B in which case the measured time delay is given by:

$$\Delta t' = \Delta t + \frac{1}{2\pi f}(2\phi_{W13} + \phi_{R13}) \quad (2)$$

where $\Phi_{W13}$ is the phase shift introduced by the transmission of A through the couplant and into the sample (B in Fig 1a), while $\Phi_{R13}$ is the phase shift introduced by the reflection of A' off the buffer rod/couplant/sample interface. The factor of 2 in the transmission term arises because the pulse returning as B has traversed the couplant layer twice and it can be shown that the phase shift introduced in this transmission is irrespective of direction (i.e. $\Phi_{W13} = \Phi_{W31}$)[5].

The reflection and transmission phase shifts are shown to be functions of (i) the characteristic impedances of the three materials: the buffer rod has impedance $z_1$, the couplant impedance $z_2$, and the sample impedance $z_3$; (ii) the magnitude of the reflection coefficient $\left|\frac{A'}{A}\right|$; and (iii) the carrier frequency of the pulse [4,5]. i.e.

$$\begin{aligned} \phi_{R13} &= \phi_{R13}(z_1, z_2, z_3, \left|\frac{A'}{A}\right|, f) \\ \phi_{R31} &= \phi_{R31}(z_1, z_2, z_3, \left|\frac{A'}{A}\right|, f) \\ \phi_{W13} &= \phi_{W31} = \phi_{W31}(z_1, z_2, z_3, \left|\frac{A'}{A}\right|, f) \end{aligned} \quad (3)$$

The phase velocity of a given acoustic wave is then given by:

$$V_p = \frac{2 * L}{\Delta t} = \frac{z_3}{\rho_3} \quad (4)$$

where $\rho_3$ is the density of the sample and the second equality follows from the definition of acoustic impedance. Equation (4) can be solved numerically for $z_3$ and the couplant corrected phase velocity thus determined.

## III. Experimental Setup

### A. Materials and preparation

LGT samples used in this work were cut and polished at the University of Maine's Microwave Acoustic Material's Lab (MAML) from a purchased boule (Fomos OAS, Moscow, Russia). Sample parallelepipeds were designed to minimize the spurious pulses due to power flow angle and mode scattering which occur along selected orientations [10]. The dimensions of the sample were measured at five different points using a length gauge (Heidenhain Corporation, Schaumburg, IL). The mean of these five measurements was used as half of the path length of an AW along that direction. The relative uncertainty in the sample dimension, $\Delta_{rel}$, is defined here as the standard deviation of the five point measurement along the orientation under consideration divided by the mean of these measurements multiplied by 100 multiplied by 2.

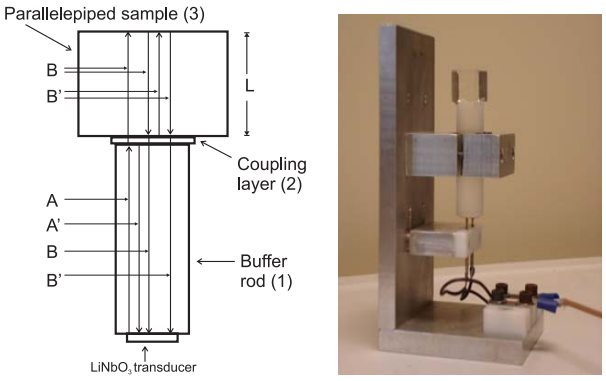


(a) (b)

Figure 1. (a) Schematic of test fixture; (b) Transducer, buffer rod, sample mounted in test fixture. Signal from RITEC generator is transmitted to transducer via pogo pins.

As depicted in Fig. 1, $LiNbO_3$ transducers were used to excite fundamental resonant modes around 6 MHz. A 36°Y rotated cut was used to excite the longitudinal modes and a 163°Y rotated cut was used to excite the shear modes. Each had a diameter of 12.0 mm and an active area 7.0 mm in diameter. The transducers were attached to a 50 mm in length and 15.0 mm in diameter silica buffer rod using an indium alloy (Indium Corporation, Utica, NY) and were not removed or changed from test to test. It is interesting to note that the exact length of the buffer rod is unimportant and adds no uncertainty to our measurements, as the transit time in the buffer rod is common to both pulses which are compared; it subtracts out of any calculations of interest.

### B. Measurement procedure

The transducer, buffer rod, and sample, shown in Fig 1b, are placed inside an oven and maintained at 25°C (+/- 0.5°C). A RITEC RAM-5000 pulse generator (Ritec Inc., Warwick, RI) is used to excite the transducers. Waveforms of the initial pulse and subsequent reflections were digitized and recorded using a LeCroy Wavepro 7100 oscilloscope (LeCroy Corporation, Chestnut Ridge, NY). For each experiment, waveforms including the original pulse created by the RITEC generator, the first reflection from the buffer rod (A' in Fig. 1a), and reflections from the back face of the cube (B, B', etc) were recorded (Fig. 2) and used for the calculation of the reflection coefficient, $\left|\frac{A'}{A}\right|$. Also recorded

were higher resolution waveforms including only the pulses used in the determination of Δt.

Fig 3 shows the high resolution (0.2 ns/point) waveform loaded into MATLAB (MathWorks, Natick, MA) and plotted on top of itself. A time offset is added to one of the pulses until the two pulses of interest overlap each other. Naturally, the time offset needed for the overlap is the delay between the two pulses, $\Delta t'$.

## IV. Results and Discussion

### A. Couplant correction validation and experimental results

Experiments with quartz, used to validate the PEO technique described above, showed that the effect of the couplant used to bond the sample to the buffer rod was greater than the experimental uncertainty and thus must be taken into account. Phase velocities for quartz determined without consideration of the couplant (PvNC) differed from those predicted by the constants in [11] by up to 0.9%, while the phase velocities determined with consideration for the couplant (PvC) agreed with those predicted by [11] to within 0.6%.

Generally, the experimental uncertainty in the phase velocity of AWs as determined by PEO is dominated by the uncertainty in the dimension of the sample. The uncertainty in the sample dimensions, as determined by the method described in Section III is ~$10^{-4}$, while the uncertainty in the time of flight is at least a whole order of magnitude smaller. The effect of applying the couplant correction to the measured data is typically on the order of $10^{-3}$ which is about an order of magnitude greater than our experimental uncertainty and thus must be considered.

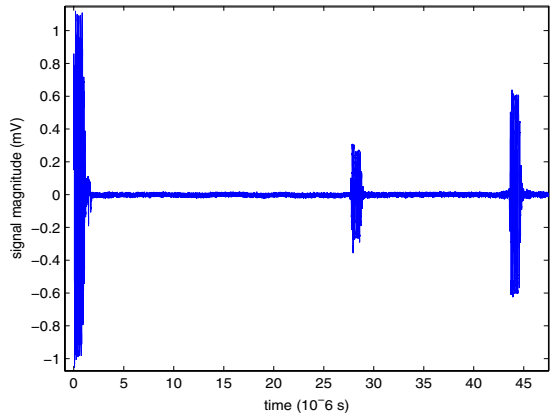


Figure 2. Waveform including initial pulse from RITEC , A', and B

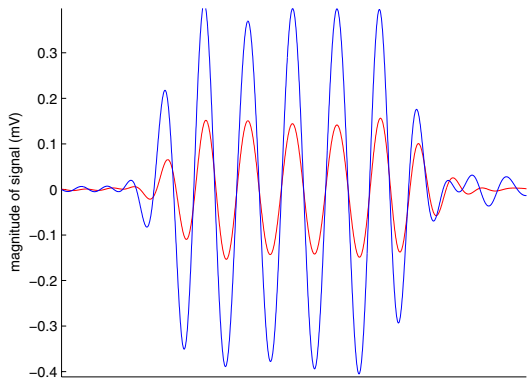


Figure 3. The overlap of two pulses of interest. While time is the unit of measure for the x axis, no numbers are given as the two pulses really correspond to two different axes.

Table 2 presents the measured LGT AW velocities before, PvNC, and after, PvC, the couplant correction has been applied. Also compared in Table 2 are the relative uncertainty in the phase velocity, $\Delta_{rel}$, dominated by the uncertainty in sample dimensions, and the correction introduced by considering the couplant, $\Delta_C$=(PvC-PvNC)/PVCC*100.

### B. Extraction of the constants and internal consistency

In extracting the material constants from the measured velocities, this work made heavy use of the redundancy of having fourteen independent equations in eight independent unknowns: the six elastic constants ($C_{11}$, $C_{13}$, $C_{14}$, $C_{33}$, $C_{44}$, $C_{66}$) and two piezoelectric constants ($e_{11}$, $e_{14}$). The method of extracting the constants was similar to that described in [9], though PEO made available two modes, the Z longitudinal and the Y+45° longitudinal, that were undeterminable in [9] through resonant techniques. The extraction of the constants in this work is outlined in Table 1. Constants providing the best internal consistency are listed in Table 3. Internal consistency is used here to describe the extent to which the extracted constants accurately predicted the phase velocities measured to extract these constants.

Table 3 compares the elastic constant values extracted in this work with constants previously published in [6], [7], & [8]. In deriving the elastic constants from the PvC, this work used values for the dielectric constants $\varepsilon_{11}$ and $\varepsilon_{33}$ from [9] and the value for the room temperature density of LGT was taken from [12]. Values extracted from the PvC for $e_{11}$ and

TABLE I. METHOD OF ELASTIC CONSTANT EXTRACTION FOR A CLASS 32 CRYSTAL

| **Constants** (in order of extraction) | **Method of extraction** (modes and other constants used) |
|---|---|
| $C_{44}$ | ZS |
| $C_{66}$ | XFS & XSS using $C_{44}$ |
| $C_{11}$ | YL & YFS using $C_{44}$ |
| $e_{11}$ | XL with $C_{11}$&$\varepsilon_{11}$<br>YSS using $C_{66}$&$\varepsilon_{11}$ |
| $C_{14}$ | XFS & XSS using $C_{44}$ & $C_{66}$<br>YL & YFS using $C_{11}$ & $C_{44}$ |
| $C_{33}$ | ZL<br>Y-45L &Y-45FS using $C_{11}$, $C_{44}$, $C_{14}$<br>Y+45L &Y+45SS using $C_{11}$, $C_{44}$, $C_{14}$ |
| $C_{13}$ | Y-45L & Y-45FS using $C_{11}$, $C_{44}$, $C_{14}$, $C_{33}$<br>Y+45L & Y+45SS using $C_{11}$, $C_{44}$, $C_{14}$, $C_{33}$ |
| $e_{14}$ | Y+45FS using $C_{14}$, $C_{44}$, $C_{66}$, $\varepsilon_{11}$, $\varepsilon_{33}$, $e_{11}$<br>Y-45SS using $C_{14}$, $C_{44}$, $C_{66}$, $\varepsilon_{11}$, $\varepsilon_{33}$, $e_{11}$ |

For modes: first letter indicates direction of propagation (X, Y, Z, Y+45°, Y-45°), second and third letters indicate mode (longitudinal, L; fast shear, FS, slow shear, SS). Along Z, only one unique shear mode, ZS, exists.

TABLE II. ACOUSTIC WAVE VELOCITIES IN LGT

| | PvNC [m/s] | PvC [m/s] | $\Delta_C$ $*10^4$ | $\Delta_{rel}$ $*10^4$ |
|---|---|---|---|---|
| XFS | 3135.3 | 3138.3 | 9.7 | 1.53 |
| XSS | 2249.2 | 2251.5 | 10.2 | 1.53 |
| ZS | 2882.2 | 2884.0 | 6.2 | 1.25 |
| XL | 5576.2 | 5576.2 | 0.0 | 1.53 |
| YL | 5561.3 | 5556.5 | -8.6 | 0.73 |
| ZL | 6527.1 | 6527.1 | 0.0 | 1.25 |
| YFS | 2845.3 | 2847.0 | 6.0 | 0.73 |
| YSS | 2604.4 | 2608.7 | 6.5 | 0.73 |
| Y+45L | 5775.6 | 5776 | 0.7 | 1.71 |
| Y-45L | 6099.0 | 6104.9 | 9.7 | 0.92 |
| Y+45SS | 3081.5 | 3083.5 | 6.5 | 1.71 |
| Y+45FS | 3110.4 | 3109.7 | -2.3 | 1.71 |
| Y-45FS | 3168.1 | 3169.5 | 4.4 | 0.92 |
| Y-45SS | 2289.1 | 2290.7 | 7.0 | 0.92 |

TABLE III. ELASTIC AND PIEZOELECTRIC CONSTANTS FOR LGT

| | This work | [7] | Δ[7] | [6] | Δ[6] | [8] | Δ[8] |
|---|---|---|---|---|---|---|---|
| $C_{11}$ | 18.85 | 18.86 | -0.06 | 18.89 | -0.21 | 18.94 | -0.48 |
| $C_{33}$ | 26.30 | 26.19 | 0.43 | 26.45 | -0.57 | 26.29 | 0.04 |
| $C_{12}$ | 10.73 | 10.79 | -0.59 | 10.86 | -1.20 | 10.84 | -1.01 |
| $C_{13}$ | 10.08 | 10.34 | -2.55 | 10.44 | -3.45 | 13.2 | -23.64 |
| $C_{14}$ | 1.36 | 1.35 | 0.52 | 1.37 | -1.16 | 1.37 | -0.88 |
| $C_{44}$ | 5.11 | 5.11 | 0.04 | 5.13 | -0.33 | 5.13 | -0.25 |
| $C_{66}$ | 4.06 | 4.03 | 0.57 | 4.02 | 0.95 | 4.05 | 0.12 |

Δ[ref] denotes the difference fractional difference between the values determined in this work and the values reported in the respective reference. (i.e. (this work – ref)/(this work)*100). Values for $C_{ij}$ are given in units of $[10^{10}$ Pa].

$e_{14}$ deviated significantly from the values published in [6-8]. The extracted value for e11 was about 20% smaller than [7], though it was only 2% smaller than [8]. The other piezoelectric constant, e14, was 2.3 times smaller than that given by [7] and more than 7.6 times smaller than [6]. These significant discrepancies with respect to previously published data suggest that additional measurements by an alternative technique, such as resonant plate, are appropriate to validate the results obtained.

## V. CONCLUSIONS

This paper reported on the significance of considering the couplant between a fused silica buffer rod and a piezoelectric crystal in performing pulse echo measurements for the extraction of elastic constants. A transmission line model has been used to model the couplant effect.

Quartz and langatate have been used in the experiments performed. Quartz has been used to validate the experimental techniques due to its well-established acoustic properties. On LGT, the BAW phase velocities of fourteen LGT AW modes along five orientations (X,Y,Z, ±45° Y rotated) were measured and from those the elastic constants determined, using an extraction technique detailed in this work.

The results obtained indicate that the influence of the couplant on the measured BAW phase velocities was about one order of magnitude higher than other experimental uncertainties. In addition, corrections for the measured BAW phase velocities on quartz and LGT were of the order of $10^{-3}$, which confirmed the necessity and relevance of the couplant effect consideration in pulse echo measurement for acoustic wave parameter extraction.

## ACKNOWLEDGMENT

The authors would like express their gratitude to the personnel from the Laboratory of Surface Science and Technology (LASST) and Dept. of Electrical and Computer Engineering for valuable technical discussion and for cutting and polishing most of the samples used in this work.

## REFERENCES

[1] H. B. Huntington, "Ultrasonic measurements on single crystals," Phys. Rev., vol 72, pp321-331, 1947.

[2] E.P. Papadakis and T.P. Learch, "Pulse superposition, pulse-echo overlap, and related techniques," in Handbook of elastic properties of solids, liquids, and gases, vol. I, Levy Bass, Stern, Eds. Academic Press, 2001, pp 39-66.

[3] D. K. Mak, "Couplant correction for ultrasonic velocity measurements," British Journal of NDT, vol 33, pp344-346, July 1991.

[4] D. K. Mak, "Ultrasonic phase velocity measurement incorporating couplant correction," British Journal of NDT, vol. 35, pp 443-449, August 1993.

[5] B. Chai, J. L. Lefaucheur, Y. Y. Ji, and H. Qiu, "Growth and evaluation of large size LGS ($La_3Ga_5SiO_{14}$), LGN ($La_3Ga_{5.5}Nb_{0.5}O_{14}$) &LGT ($La_5Ga_{5.5}Ta_{0.5}O_{14}$) single crystals," Proc. 1998 IEEE Int'l. Freq. Cont. Symp., pp 748-760.

[6] J. Bohm, E. Chilla, C. Flannery, H.J Frohlich, T. Hauke, R.B. Heimann, M. Hengst, U. Straube, "Czochralski growth and characterization of piezoelectric single crystals with langasite structure: $La_3Ga_5SiO_{14}$ (LGS), $La_3Ga_{5.5}Nb_{0.5}O_{14}$ (LGN) and $La_3Ga_{5.5}Ta_{0.5}O_{14}$ (LGT) II. Piezoelectric and elastic properties," Journal of Crystal Growth, 216, pp 293-298, 2000.

[7] M. Pereira da Cunha, D. C. Malocha, E. L Adler, K. J. Casey, "Surface and pseudo surface acoustic waves in langatate: predictions and measurements," IEEE Trans. Ultrason., Ferroelect., Freq. Cont., vol 49, pp 1291-1299, September 2002.

[8] Y. V. Pisarevsky, P.A. Senyushenkov, B.V. Mill, N.A. Moiseeva, "Elastic, Piezoelectric, Dielectric Properties of La3Ga5.5Ta0.5O14 Single Crystals," Proc. 1998 IEEE Int'l. Freq. Cont. Symp., pp 742-747.

[9] P. Davulis, J. A. Kosinski, M. Pereira da Cunha, "GaPO4 stiffness and piezoelectric constants measurements using the combined thickness excitation and lateral field technique," Proc. 2006 IEEE Int'l Freq. Cont. Symp., in press

[10] B. J. Meulendyk, M. Pereira da Cunha, "Significance of power flow angle interference due to finite sample dimensions in reflection measurements," Proc. 2005 IEEE Int'l. Freq. Cont. Symp., pp 164-170.

[11] B. J. James, "A new measurement of the basic elastic and dielectric constants of quartz," Proc. 1988 IEEE Int'l. Freq. Cont. Symp. pp 146-154.

[12] T. R Beaucage, E.P Beenfeldt, S.A Speakman, W.D Porter, E.A. Payzant, M.Pereira da Cunha, "Comparison of high temperature crystal lattice and bulk thermal expansion measurements of LGT single crystal," Proc. 2006 IEEE Int'l Freq. Cont. Symp., in press